An *in vitro* blood–brain barrier model: Cocultures between endothelial cells and organotypic brain slice cultures

(glutamate/picrotoxin/dopamine/L-dopa/tight junction)

S. DUPORT*, F. ROBERT*, D. MULLER*, G. GRAU†, L. PARISI*, AND L. STOPPINI*‡

Departments of *Pharmacology and †Anesthesiology and Intensive Care, Centre Médical Universitaire, CH-1211 Geneva 4, Switzerland

ABSTRACT This communication describes a novel *in vitro* blood–brain barrier (BBB) model: organotypic slice cultures from the central nervous system were overlaid on endothelial cell monolayers grown on permeable membranes. Morphological, electrophysiological, and microdialysis approaches were carried out to characterize and validate this model. After 10 days in coculture, morphological studies reveal the presence of tight junctions. Electrophysiological recordings of neuronal activity performed on organotypic cultures with or without an endothelial cell monolayer show that amplitude of evoked responses were comparable, indicating good viability of cocultures after 2 weeks. Perfusion of known BBB permeable or nonpermeable molecules was used to test the coculture tightness in conjunction with electrophysiological or microdialysis approaches: application of glutamate (Glu), which doesn't easily cross the BBB, triggers off rhythmic activity only in control cultures, whereas epileptogenic activity was observed in both control cultures and cocultures during perfusions with picrotoxin, a molecule that can diffuse through the BBB. Finally, the microdialysis technique was used to determine the permeability of molecules coming from the perfusion chamber: L-dopa, dopamine, and Glu were employed to assess the selective permeability of the coculture model. Thus, these results indicate that the *in vitro* model described possesses characteristics similar to those of the BBB *in situ* and that cocultures of organotypic slices and endothelial cell monolayers have potential as a powerful tool for studying biochemical mechanisms regulating BBB function and drug delivery to the central nervous system.

The microenvironment of the central nervous system (CNS) is important for neuronal function. In this context, the blood–brain barrier (BBB) provides and maintains the extracellular medium compatible with normal neuronal activity. Through multiple studies, the characteristics of the BBB in mammals were found to be due to cerebral endothelial cells. Among these characteristics, the presence of tight junctions (TJs), the selective permeability, and the polarity were found to be essential for a functional BBB (1–3).

The difficulties inherent to the use of whole animals as experimental models for studying permeability and metabolic processes at the cellular level has led to major efforts in the last decades to design suitable *in vitro* models. Three prototypes are noteworthy: the first consists of suspensions of isolated microvessels obtained from cerebral cortex gray matter (4–7). The second was developed following the demonstration by Panula *et al.* (8) that brain endothelial cells could be maintained in culture. In this model, primary passage cultures and clones (9, 10) of isolated brain endothelial cells were used as

an *in vitro* BBB (11–13). The third was provided by the work of Stewart and Willey (14) and Janzer and Raff (15) on the importance of the cellular environment of endothelial cells. As a consequence, it has been possible to simulate a BBB *in vitro* by coculturing astrocytes and endothelial cell monolayers on plastic (16, 17) or on either side of filters (18–22).

The role of neurons to induce and to maintain BBB properties of endothelial cells, although not fully determined, is certainly of paramount importance. Neurons may directly influence endothelial cell permeability or may indirectly act on BBB properties by modifying glial cells' characteristics (23, 24). We propose a new model of *in vitro* BBB made of complex organized nervous tissue that contains the different cells normally present in the nervous parenchyma placed over confluent endothelial cell monolayers. Neuronal architecture and electrophysiological activity in organotypic slice culture were found to be similar to their *in situ* counterpart (25–27). Thus, in coculture with endothelial cell monolayers, stationary organotypic slice cultures represent an easy means to realize an *in vitro* BBB model that mimics as closely as possible the *in vivo* situation. Morphological, electrophysiological, and microdialysis approaches were carried out to characterize and to validate this model.

MATERIALS AND METHODS

Coculture Protocol. Cerebrovascular microvessels were isolated by modification of the technique developed for bovine brain (11). After removing brains from 7-day-old rats or mice, meninges and macroscopic pial vessels were taken off. The cortex were dissected, the tissue was minced in dissection medium (MEM) and mixed with a 0.1% collagenase solution overnight at 4°C. Fragments of tissue were centrifuged at 1,500 × *g* for 5 min and the pellet was resuspended in 5 ml of dissection medium. The cell suspension was then centrifuged in a 20% Percoll gradient. The pellet was washed and cells were seeded onto culture-grade plastic flasks containing 5 ml of endothelial cell culture medium [15% horse serum/10% fetal calf serum/Endothelial cell growth supplement (0.1 μg/ml)/ 50% MEM/25% Hanks' solution]. Endothelial cells were grown in a 5% CO_2/95% air incubator at 37°C. Endothelial cell purity was determined by an immunostaining for factor VIII-related antigen, and the presence of remaining glial cells was detected by glial fibrillary acidic protein labeling. When endothelial cells reached confluence, they were dissociated by enzymatic digestion (1% trypsin/EDTA), collected, and seeded (10^5 cells per mm^2) onto collagen-treated patches of transparent and porous membrane (Millipore CM, 0.45 μm, pore size). After 3 days in culture, confluent monolayers were generated.

Hippocampal slices from 7-day-old rats were kept in culture for 1 week to allow tissue recovery from explantation trauma as described (25). Slices were then carefully taken off and laid on top of endothelial cell monolayers. Great care was taken to ensure that the previous membrane side of the slice was effectively in contact with endothelial cells. From previous experiments (25), we know that glial cells are more abundant in the lower part of the organotypic culture, this particular tissue culture reorganization, therefore, favors glial–endothelial cell contacts. Coculture assemblies were normally used for experiments 4–10 days after their coupling. The coculture model is schematically represented in Fig. 1*A*. Hippocampus slices are laid onto confluent endothelial cell monolayers grown on permeable membranes. The culture medium is added underneath the membrane so it has to cross the synthetic membrane and the endothelial cell monolayer before reaching the nervous parenchyma.

Histological and Morphological Analyses. The morphology of endothelial cell monolayers was investigated in conventional or in freeze–fracture electron microscopy.

Preparation for Conventional Electron Microscopy. Slices were briefly rinsed in 0.1 M sodium phosphate (pH 7.4) and fixed with a solution of 3% glutaraldehyde and 2% paraformaldehyde in 0.1 M sodium phosphate (pH 7.4) for 2 h at 4°C. The slices were then rinsed in phosphate buffer and postfixed in osmium for 1 h. After three more rinses in phosphate buffer, samples were dehydrated through an ascending series of ethanol concentrations, placed into a graded propylene oxide/Epon mixture and left overnight in Epon. The slices were first flat-embedded in Epon between transparent plastic foils for 48 h at 60°C. Blocks were then embedded again in gelatin

capsules. Semithin sections were then briefly stained with a diluted aqueous solution of methylene blue and azur II and mounted to visualize the coculture by using light microscopy. Ultrathin sections of 50–70 nm were mounted on uncoated copper grids and stained with aqueous uranyl acetate and lead citrate. The sections were examined with a Philips CM10 electron microscope at 80 kV.

Preparation for Freeze Fracture. The procedure was adapted from the flatten-peeled technique described by Corrèges *et al.* (28). Briefly, the specimen is flattened overnight between two membranes treated with poly-(L-lysine). The membrane above the tissue is peeled to break apart the different levels of the tissue. This technique permits a larger surface of endothelial membranes to be fractured, enhancing the visualization of interendothelial contact areas.

Endothelial Cell Monolayer's Permeability. Ionic lanthanum forms an electron-dense precipitate with phosphate and hence is useful as an electron microscopical tracer for ion permeability at the BBB (29, 30). Cocultures were initially perfused with phosphate-free Tris-buffered artificial cerebrospinal fluid for 5–10 min, to wash out excess phosphates, followed with perfusion by 20 mM lanthanum chloride (LaCl$_3$, Sigma) in the same artificial cerebrospinal fluid for up to 15 min. Cultures were fixed for 90 min with phosphate-buffered fixative containing 2% paraformaldehyde and 3% glutaraldehyde, a procedure that causes La^{3+} to precipitate. Tissues were then processed for electron microscopy.

Electrophysiology. Cultures were placed in an interface-type chamber, gassed with a humid atmosphere composed of 95% O$_2$/5% CO$_2$, and continuously perfused with an artificial medium containing 124 mM NaCl, 3 mM KCl, 2.5 mM CaCl$_2$,
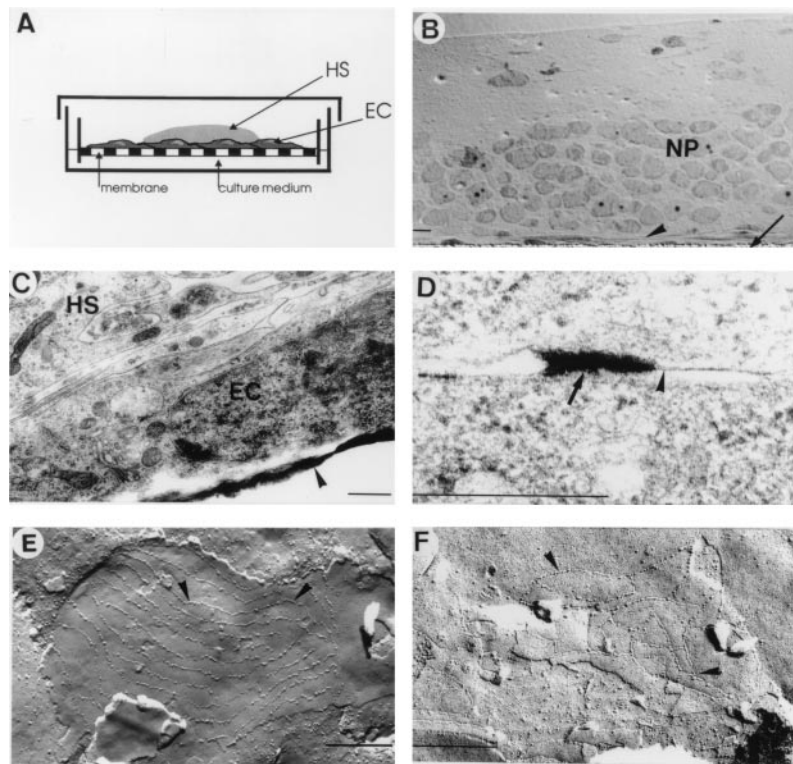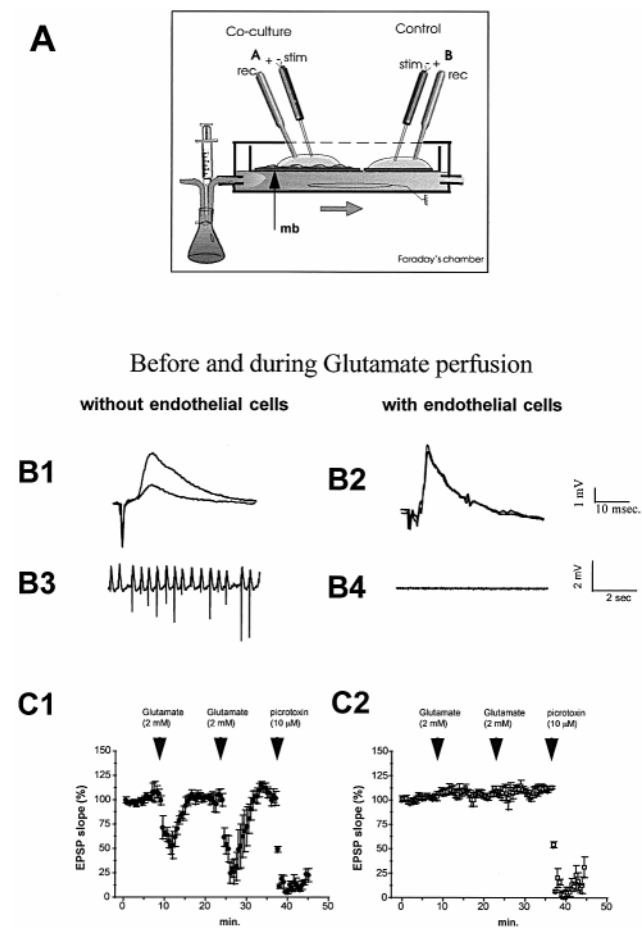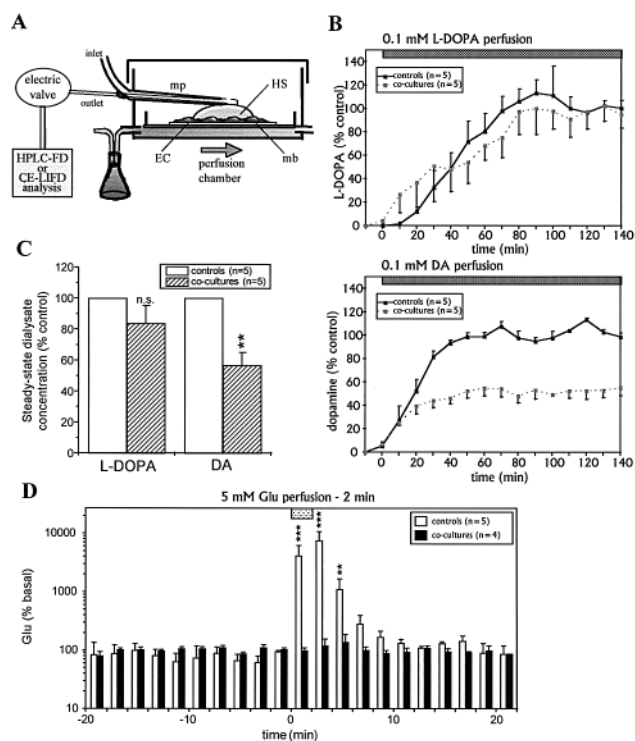

FIG. 1. (*A*) Schematic representation of a coculture assembly. An organotypic hippocampal slice (HS) was laid down onto a confluent endothelial cell monolayer (EC) grown on a porous membrane. Culture medium was added only below the membrane insert. (*B*) Transversal semithin section of a coculture observed in light microscopy. The membrane insert is indicated by an arrow. The endothelial cell monolayer (arrowhead) and the neuropil (NP) are in close contact. (Bar = 10 μm.) (*C*) Electron microscopic microphotography of a transversal section of a coculture showing a piece of membrane insert (arrowhead), an endothelial cell (EC), and glial filopodia from the hippocampal slice culture (HS). (*D*) Accumulation of ionic lanthanum (arrow) near joining membranes of endothelial cells (arrowhead) was observed in electron microscopic microphotography. (*E* and *F*) Microphotographies of freeze–fracture replica of 10 days cocultures. (*E*) TJs can be identified by typical long strand structures (arrowheads). Those strands can sometimes be linked together, whereas in *F* the TJ is composed by a proper net of short strands. (Bars = 0.5 μm.)

1.5 mM $MgCl_2$, 26 mM $NaHCO_3$, 1.25 mM KH_2PO_4, 2 mM ascorbic acid, and 10 mM glucose (pH 7.4). The temperature was maintained at 34°C by warming a bath filled with distilled water. The cultures could be kept for several hours in this chamber. Stimulation electrodes made of twisted nichrome wires were placed on a group of CA3 neurons of the hippocampus, and synaptic responses were recorded extracellularly by using pipettes filled with saline solution (about 5 MΩ resistance) in the CA2–CA1 region. Two cultures (control culture and coculture) were stimulated simultaneously. Spontaneous and evoked synaptic activities were recorded. Bolus of Glu (final concentration, 2 mM) and picrotoxin (10 μM) were perfused underneath the membrane in the lower part of the recording chamber (Fig. 2*A*).

Microdialysis. Side-by-side microdialysis probes were made from fused-silica capillary tubing (105 μm, o.d.; 40 μm, i.d.) and cellulose dialysis tubing (225 μm, o.d.; 2 mm, active dialysis length). Probes were delicately placed onto the surface of the hippocampal slice (Fig. 3*A*). In these conditions, lesions produced by the insertion of the microdialysis probe are limited to

FIG. 2. (*A*) Scheme of the experimental electrophysiological set-up. A coculture (*A*) or a control culture (*B*) were simultaneously stimulated and recorded in an interface-type chamber. Perfusion medium flows beneath the membrane insert (mb). (*B1* and *B2*) Representative field potentials recorded in the pyramidal layer before and after Glu perfusion in control cultures and cocultures. Note the important decreasing in EPSP responses occurring for Glu perfusion in control cultures (*B1*). Rhythmic activity was observed when recording spontaneous activity during Glu perfusion (*B3*). No modification of either evoked responses (*B2*) or spontaneous activity (*B4*) was observed in cocultures (*n* = 4). (*C1*) Synaptic responses (slope of EPSP, percent) in control cultures (*n* = 4) before and during perfusions of Glu and picrotoxin. EPSP decreasing was observed only when picrotoxin was perfused in coculture experiments (*C2*).

FIG. 3. (*A*) Scheme of the microdialysis set-up. Microdialysis probes were put down onto control or coculture slices. Artificial cerebrospinal fluid solution was continuously perfused (1 μl/min). The molecules of interest were perfused continuously (L-dopa and dopamine) or perfused for a 2-min period (Glu) below the membrane insert supporting the slice. The concentrations of these compounds in the microdialysates were determined by using HPLC system with fluorimetric detection (for L-dopa and dopamine) or capillary electrophoresis with laser-induced-fluorescence detection (for Glu). (*B*) Kinetics of L-dopa (*Upper*) and dopamine (*Lower*) collected by a microdialysis probe in control (continuous line) or in coculture (dotted line) experiments. (*C*) Concentrations of L-dopa and dopamine reached during the steady state in the control and cocultures experiments presented in *B*. (*D*) Kinetics of Glu collected by a microdialysis probe in control or in coculture experiments. Data are the mean ± SEM of steady-state values in the control slices (L-dopa and dopamine) or basal values (Glu). mp, Microdialysis probe.

the superior part of the slice and are insignificant when compared with those occurring *in vivo*. The inlet of the dialysis probe was connected to a perfusion pump, and the outlet was attached to the appropriate analysis system. The probes were continuously perfused with a modified Ringer's solution of the following composition: 124 mM NaCl, 1.6 mM KCl, 2.5 mM $CaCl_2$, 1.5 mM $MgCl_2$, 1.2 mM KH_2PO_4, 25 mM Tris, 10 mM glucose, and 25 mM Hepes (pH 7.4) at a flow rate of 1 μl/min. The probe recovery was found to be about 8% because of the low active dialysis membrane surface in contact with the tissue.

For dopamine and L-dopa permeability experiments, the probe outlet was connected to the automatic injection valve of an HPLC system with fluorimetric detection. Ten-minute fractions were collected and automatically analyzed by using the on-line HPLC system. The permeability test consisted of a continuous perfusion of dopamine and L-dopa (both 0.1 mM) through the culture medium chamber while the on-line HPLC system was used to assess kinetics of catecholamines diffusion.

For Glu permeability experiments, the probe outlet was connected to a continuous flow derivatization system, as described (31–33). This system allows us to perform the derivatization step on very low sample volumes and thus permits high temporal resolution of the microdialysis approach (up to 30-s fractions). In the present study, 2-min fractions were collected for further analysis. An internal standard

(α-amino adipic acid) was added to correct variations appearing during derivatization and injection steps. The permeability test consisted in a 2-min perfusion of Glu (5 mM) through the culture medium chamber while the kinetics of Glu diffusion was assessed by capillary electrophoresis with laser-induced-fluorescence detection analysis.

Analysis of Dialysates. For dopamine and L-dopa, a reversed-phase HPLC with a fluorimetric detection system was used, consisting of a model PU980 HPLC pump (Jasco, Easton, MD), a Valco automatic injector equipped with a 10-μl sample loop, a Spheri 5 RP18 column (100 × 4.6 mm i.d., Macherey & Nagel) and a model FP920 fluorimeter (Jasco) with an excitation wavelength of 275 nm and an emission wavelength of 317 nm. The mobile phase contained 12.8 mM sodium acetate, 0.37 mM octanylsulfonic acid, 0.46 mM EDTA, and 15% (vol/vol) methanol and was adjusted at pH 3 with acetic acid. The separation was accomplished at +40°C at a flow rate of 0.5 ml/min.

For Glu determination, capillary electrophoresis was performed on a Spectraphoresis 100 module purchased from Thermo Separation Products (Les Ulis, France) equipped with a laser-induced-fluorescence detector from Zeta Technology (Toulouse, France), as described (33). Briefly, the excitation was performed by an Omnichrome (China, CA) helium–cadmium laser at a wavelength of 442 nm. The emission intensity was measured at a wavelength of 490 nm. Separations were carried out with a fused-silica capillary with a 50-μm i.d., a 375-μm o.d., a total length of 60 cm, and an effective length of 20 cm (defined as the length from the point of injection to the point of detection). On-column laser-induced-fluorescence detection was carried out through a 5-mm-wide window opened by removing the polyimide cover of the capillary. The separation buffer used was 100 mM borate buffer (pH 9.2) and the running voltage was 27 kV. Electrokinetic injections were performed by making contact between the capillary and the sample and applying running voltage.

RESULTS

Morphological Analyses of the Coculture Assembly. Excellent survival of the CNS-derived slice tissue constitutes the corner stone of the model. Because mature neurons are very sensitive to minor environment variations, it was, therefore, important to verify whether in coculture conditions insertion of endothelial cell monolayers does not compromise the fragile balance among gas diffusion, culture medium, and the slice tissue. After 1 week in coculture, tissues were fixed and processed for electron microscopy. Transversal semithin sections of cocultures observed in light microscopy revealed good nervous tissue survival and the presence of an endothelial cell monolayer between the membrane and the neuropil (Fig. 1*B*). Electron microscopy studies confirmed the integrity of the nervous parenchyma and delineate glial filopodia contacting endothelial cell membranes (Fig. 1*C*). In control cultures, numerous inflammatory cells were localized between the synthetic membrane and the nervous parenchyma (data not shown). In contrast, after 1 week in coculture, most of these cells have disappeared and endothelial cells were found in direct contact with the neuropil (Fig. 1 *B* and *C*).

When ionic lanthanum, a small electron-dense tracer, is perfused in the blood stream, it is stopped at the TJ in most instances (29, 34). Thus, this tracer was used to assess the extracellular permeability of the *in vitro* model. After the perfusion of lanthanum solution, accumulations of ionic lanthanum were present near interendothelial junctions in the coculture assembly, but no deposit was observed in the nervous parenchyma of the coculture or in the control culture (Fig. 1*D*).

Our freeze–fracture technique gives access to the intermembrane particles, by separating the different leaflets of the membrane. Both types of particle assembly characteristic for TJs were found after 1 week in the coculture model but not in confluent endothelial monolayer alone. Fig. 1*E* illustrates the long strands sparsely linked together, and Fig. 1*F* shows short strands with multiple links among themselves, forming a complex network assembly.

Electrophysiology. The recording of synaptic activity (excitatory postsynaptic potential, EPSP) from the extracellular medium was used as an indicative means to assess the permeability of the BBB to neuroactive solutes. Amplitude of evoked responses serves as an indication of the overall electrical activity of neurons. When spontaneous rhythmic activities (seizures) were elicited (e.g., by using epileptogene molecules or intense stimulation), evoked responses are diminished or completely abolished. Two types of epileptogenic molecules were tested: Glu, for its low BBB permeability, and picrotoxin (a γ-aminobutyric acid antagonist) for its high BBB permeability. A bolus of Glu (final concentration, 1–2 mM) induced seizures in control cultures (without endothelial cells), which resulted in an important diminution of amplitudes of evoked responses (Fig. 2*B1*), but no change was observed in the endothelial–nervous slice coculture assembly (Fig. 2*B2*). Spontaneous neuronal activity during Glu perfusion is illustrated in Fig. 2 *B3* and *B4*. Rhythmic activity was observed in control cultures (Fig. 2*B3*) but not in cocultures (Fig. 2*B4*).

Fig. 2 *C1* and *C2* show the changes in slope of the synaptic responses recorded in control cultures and in cocultures (n = 4) before and during perfusion of Glu or picrotoxin. A decrease of the EPSP slope was observed when Glu was perfused in control cultures, whereas no change was detected in cocultures. Shortly after recovery of the response, a second perfusion of Glu gave a similar result. After the control culture recovery, picrotoxin (10 μM) was perfused and a dramatic rhythmic activity was elicited with an almost complete abolition of evoked responses in both control cultures (Fig. 2*C1*) and coculture assemblies (Fig. 2*C2*).

Microdialysis. To determine the permeability of the BBB model, we developed an *in vitro* microdialysis system for organotypic slice cultures that allows the monitoring of the diffusion of exogenous molecules through the slices. Molecules with different BBB permeabilities were perfused through the culture medium chamber and their concentrations were determined in brain slices microdialysates. First, the simultaneous perfusion of the neurotransmitter dopamine and its precursor L-dopa induced their appearance in dialysates. After 30 and 70 min, respectively, a steady-state was reached that was not statistically different for L-dopa in control and in cocultures experiments (83.8 ± 11.8% of control values), whereas only 50.8 ± 6.9% of the control dopamine concentration was present in microdialysates collected from coculture assemblies ($P < 0.01$, Student's t test, n = 5 for each group; Fig. 3*B* and *C*). Therefore, the differential BBB permeability between L-dopa and dopamine found *in vivo* is also observed in the coculture. Finally, a 2-min perfusion of Glu induced a very large increase of Glu concentrations in dialysates from control slices (maximal increase: +7400% at +4 min; Fig. 3*D*). This increase was totally prevented when such a perfusion was performed on cocultures (maximal increase: +36% at +4 min; Fig. 3*D*), showing no passing of Glu through the BBB model.

DISCUSSION

In vitro BBB models are important tools to study cellular events leading to the induction of some BBB properties (16, 17, 35–40). In the majority of existing models, glial–endothelial cell relationships were found to be of fundamental importance for establishing a restricted permeability similar to that of the *in vivo* BBB (41–44). Data from Tontsch *et al.* (45) provide direct evidence that the establishment of metabolic and structural properties of the BBB involves not only glial cells but also

neurons through cell–cell contact with endothelial cells during cerebral ontogenesis. By examining the developmental spatio-temporal expression of different BBB markers, Dermietzel and Krause (23) concluded that the mechanisms governing the pattern of BBB maturation are not limited to the interactions occurring between glial and endothelial cells. They therefore suggest a triangular interrelationship that includes differentiation effects of neurons on glia and of glia cells on the BBB endothelium. The aim of the present study was to develop an *in vitro* model that takes into account the complex environment of the brain.

Three complementary approaches (morphology, electrophysiology, and microdialysis) were used to characterize and validate this *in vitro* BBB model.

No morphological difference was found between control cultures and cocultures at the neuronal level. No inflammatory reaction between endothelial cells and the nervous parenchyma was observed.

Ionic lanthanum has been used successfully in a number of investigations as a vascular probe to study endothelial BBB, because of its high permeability, small size, and nontoxic properties (34, 46). In our study, we could observe lanthanum precipitates filling intercellular clefts, the diffusion of the ion being stopped at the interendothelial level. This restriction of pathway prevents diffusion of the tracer into the neuropil. Because La^{3+} was stopped in the coculture at the endothelial level and not stopped at all in the control culture, we may conclude that our model possesses a greater extracellular tightness at the endothelial level.

Tight intercellular junctions constitute the anatomical basis of the selective permeability of the BBB (47–50). Thus, the first part of this work was devoted to the characterization of the coculture's morphology to reveal whether TJs were present in this model. Freeze–fracture electron microscopy reveals intramembrane structure. With this technique, TJs appear as long parallel linear fibrils that circumscribe the cell, with short fibril fragments interconnecting the main parallel array (51). TJs observed in freeze–fracture replica of cocultures displayed similar structures and organization to those described in *in vitro* BBB models (16, 52–54). Moreover, in our cocultures, TJs exhibit the morphological appearance found in brain microvessels with strands forming complex networks (55, 56).

In the proposed *in vitro* model, neurons can also be used as biosensors to detect the presence of neuroactive molecules, besides to their potential role in BBB formation. Thus, electrophysiological recording of neuronal activity represents another means to assess the selective permeability of the BBB. Neuronal activity in hippocampal organotypic cultures or acute slices is well documented (25, 26, 57–59), and modification of extracellular responses to epileptogenic molecules can be easily recognized by (*i*) a diminution of EPSP amplitudes and (*ii*) an apparition of rhythmic (synchronous) activity (60, 61). Glu and picrotoxin, two molecules known for their seizure-induction property when applied on hippocampal slices, were tested in the coculture model. Like several others CNS transmitters, Glu is prevented by the BBB from entering most brain regions from blood, and this agent is rapidly removed from the extracellular compartment by a Na^+-dependent high-affinity uptake system that is believed to terminate the action of these agents at excitatory synapses (62–66). As Glu concentration can be 1,000-fold higher in the blood than in the extracellular space of the brain, a barrier to this amino acid is essential to allow a normal neuronal and synaptic activity (1). In contrast, picrotoxin, a γ-aminobutyric acid antagonist, can easily cross the BBB and can induce epilepsy in animals (67, 68). Our results indicate that Glu was prevented from reaching the nervous tissue in the coculture assemblies, whereas the picrotoxin epileptogenic effect was observed, as expected, in both control and cocultures.

The confirmation of the selective permeability of this *in vitro* model was achieved by the means of the microdialysis technique (69, 70). Intracerebral microdialysis is an *in vivo* technique by which concentrations of small endogenous compounds can be monitored dynamically (71, 72). More recently, applications in the field of pharmacokinetics have been reported (73–75), where microdialysis has appeared as a powerful tool to investigate BBB transport (76, 77). We previously described an application of the microdialysis technique for monitoring changes in Glu release on hippocampal organotypic slice cultures (33). Herein, we have adapted this approach to monitor the diffusion of molecules from the perfusion chamber to the nervous tissue. The results obtained in this study show that a barrier to dopamine penetration was present in coculture by comparison to control culture. Indeed, in contrast to dopamine, L-dopa can diffuse through endothelial cells probably by taking advantage of large neutral amino acid transport system.

The use of capillary electrophoresis with laser-induced-fluorescence detection as an alternative technique for the determination of Glu in microdialysis samples allows us to reach high temporal resolution (up to 30 s; refs. 33 and 78). Subtle changes in extracellular Glu can thus be monitored, allowing the administration of a bolus of Glu for a short time period (2 min) to mimic the experimental protocol used in the electrophysiological studies. The microdialysis data obtained for Glu confirm the very selective permeability of the *in vitro* BBB model shown in the electrophysiological studies.

The proposed model takes advantage of the characteristics of the interface type of organotypic cultures where organized nervous tissues can be maintained alive and are allowed to mature *in vitro* when placed onto permeable membranes (25–27). By interfacing endothelial cells, the system consists of two compartments representing the luminal and the abluminal side of the BBB. A unique aspect of this model is the preservation of the different cells' types and the three-dimensional organization of the nervous tissue. As a consequence, diffusion of molecules should occur in a compact parenchyma, as it happens *in vivo*. TJs were found only in presence of the nervous tissue, suggesting that the hippocampal slice may have an influence on BBB formation either by direct contact or by release of diffusible factor(s).

During this study, some difficulties inherent to our system were encountered. The proportion of unsuccessful cultures was found to be one per four tested preparations (between 25 and 30% of failure). The measurement of the electrical conductance of the endothelial layer should be a quicker way to reject unsuitable cocultures.

Despite these drawbacks, our system has a number of unique advantages: (*i*) it allows simple and quick preparations of more than one coculture at a time by using a three-dimensional neural tissue, (*ii*) precise positioning of the microdialysis probe without breaking the BBB, (*iii*) electrophysiological recordings give immediate information on drug permeability and neurotoxicity, and (*iv*) the use of small amounts of drugs and the precise control of the environment represent advantages compared with *in vivo* approaches. In addition, different CNS regions from wild-type or transgenic animals can be cocultured with endothelial cells from different origin/developmental states. These combinations open up possibilities for studying pathological processes (epilepsy, ischemia, inflammation, and hypoxia).

In summary, we provide evidence that cocultures of organotypic slices and endothelial cell monolayers possess similar characteristics to *in situ* BBB. This *in vitro* model should be a useful tool to assess drug permeabilty and to reveal factors that influence the activity of the endothelial cells in their maintenance of a constant environment for the brain.

1. Villegas, J. C. & Broadwell, R. D. (1993) *J. Neurocytol.* **22,** 67–80.
2. Pardridge, W. M. & Oldendorf, W. H. (1977) *J. Neurochem.* **28,** 5–12.
3. Betz, A. L., Firth, J. A. & Goldstein, G. W. (1980) *Brain Res.* **192,** 17–28.
4. Betz, A. L. & Golstein, G. W. (1978) *Science* **161,** 370–371.
5. Bowman, P. D., Ennis, S. R., Rarey, K. E., Betz, A. L. & Goldstein, G. W. (1983) *Ann. Neurol.* **14,** 396–402.
6. Matsumura, K., Abe, I., Fukuhara, M., Tominaga, M., Tsuchihashi, T., Kobayashi, K. & Fujishima, M. (1994) *Am. J. Physiol.* **266,** R1403–R1410.
7. Abbott, N. J., Hughes, C. C., Revest, P. A. & Greenwood, J. (1992) *J. Cell Sci.* **103,** 23–37.
8. Panula, P., Joo, F. & Rechardt, L. (1978) *Experientia* **34,** 95–97.
9. Durieu Trautmann, O., Foignant Chaverot, N., Perdomo, J., Gounon, P., Strosberg, A. D. & Couraud, P. O. (1991) *In Vitro Cell. Dev. Biol.* **27A,** 771–778.
10. Begley, D. J., Lechardeur, D., Chen, Z. D., Rollinson, C., Bardoul, M., Roux, F., Scherman, D. & Abbott, N. J. (1996) *J. Neurochem.* **67,** 988–995.
11. Audus, K. L. & Borchardt, R. T. (1986) *Pharm. Res.* **3,** 81–87.
12. Furie, M., Cramer, E., Naprstek, B. & Silverstein, S. (1984) *J. Cell Biol.* **98,** 1033–1041.
13. Joo, F. (1992) *J. Neurochem.* **58,** 1–17.
14. Stewart, P. A. & Wiley, M. (1981) *Dev. Biol.* **84,** 183–192.
15. Janzer, R. C. & Raff, M. C. (1987) *Nature (London)* **325,** 253–257.
16. Arthur, F. E., Shivers, R. R. & Bowman, P. D. (1987) *Brain Res.* **433,** 155–159.
17. Laterra, J., Guerin, C. & Goldstein, G. (1990) *J. Cell Physiol.* **144,** 204–215.
18. Beck, D. W., Vinters, H. V., Hart, M. N. & Cancilla, P. A. (1984) *J. Neuropathol. Exp. Neurol.* **43,** 219–224.
19. Dehouck, M. P., Meresse, S., Delorme, P., Fruchart, J. C. & Cecchelli, R. (1990) *J. Neurochem.* **54,** 1798–1801.
20. Raub, T. J., Kuentzel, S. L. & Sawada, G. A. (1992) *Exp. Cell Res.* **199,** 330–340.
21. Biegel, D. & Pachter, J. S. (1994) *In Vitro Cell. Dev. Biol. Anim.* **30A,** 581–588.
22. Deli, M. A. & Joo, F. (1996) *Keio J. Med.* **45,** 183–198.
23. Dermietzel, R. & Krause, D. (1991) *Int. Rev. Cytol.* **127,** 57–109.
24. de Boer, A. G. & Breimer, D. D. (1994) *J. R. Coll. Physicians Lond.* **28,** 502–506.
25. Stoppini, L., Buchs, P. A. & Muller, D. (1991) *J. Neurosci. Methods* **37,** 173–182.
26. Muller, D., Buchs, P. A. & Stoppini, L. (1993) *Brain Res. Dev. Brain. Res.* **71,** 93–100.
27. Buchs, P. A., Stoppini, L. & Muller, D. (1993) *Brain Res. Dev. Brain. Res.* **71,** 81–91.
28. Corrèges, P., Sors, P. & Dunant, Y. (1996) *Microsc. Res. Tech.* **34,** 478–487.
29. Xu, J. & Ling, E. A. (1994) *J. Anat.* **184,** 227–237.
30. Bundgaard, M. (1982) *Brain Res.* **241,** 57–65.
31. Bert, L., Robert, F., Denoroy, L., Stoppini, L. & Renaud, B. (1996) *J. Chromatogr. A* **755,** 99–111.
32. Robert, F., Bert, L., Lambas-Senas, L., Denoroy, L. & Renaud, B. (1996) *J. Neurosci. Methods* **70,** 153–162.
33. Robert, F., Parisi, L., Bert, L., Renaud, B. & Stoppini, L. (1997) *J. Neurosci. Methods* **74,** 65–76.
34. Hirano, A., Kawanami, T. & Llena, J. F. (1994) *Microsc. Res. Tech.* **27,** 543–556.
35. Pardridge, W. M., Triguero, D., Yang, J. & Cancilla, P. A. (1990) *J. Pharmacol. Exp. Ther.* **253,** 884–891.
36. Rubin, L. L., Hall, D. E., Porter, S., Barbu, K., Cannon, C., Horner, H. C., Janatpour, M., Liaw, C. W., Manning, K., Morales, J. & *et al.* (1991) *J. Cell. Biol.* **115,** 1725–1735.
37. Joo, F. (1993) *Neurochem. Int.* **23,** 499–521.
38. Bree, J. M., Boer, A. G., Danhof, M., Ginsel, L. A. & Breimer, D. D. (1988) *J. Exp. Pharmaco. Exp. Ther.* **247,** 1233–1239.
39. Jaehde, U., Masereeuw, R., de Boer, A. G., Fricker, G., Nagelkerke, J. F., Vonderscher, J. & Breimer, D. D. (1994) *Pharm. Res.* **11,** 442–448.
40. Lane, N. J., Revest, P. A., Whytock, S. & Abbott, N. J. (1995) *J. Neurocytol.* **24,** 347–360.
41. Minakawa, T., Bready, J., Berliner, J., Fisher, M. & Cancilla, P. A. (1991) *Lab. Invest.* **65,** 32–40.
42. Rauh, J., Meyer, J., Beuckmann, C. & Galla, H. J. (1992) *Prog. Brain Res.* **91,** 117–121.
43. Dehouck, M. P., Jolliet Riant, P., Bree, F., Fruchart, J. C., Cecchelli, R. & Tillement, J. P. (1992) *J. Neurochem.* **58,** 1790–1797.
44. Hurwitz, A. A., Berman, J. W., Rashbaum, W. K. & Lyman, W. D. (1993) *Brain Res.* **625,** 238–243.
45. Tontsch, U. & Bauer, H. C. (1991) *Brain Res.* **539,** 247–253.
46. Butt, A. M., Jones, H. C. & Abbott, N. J. (1990) *J. Physiol. (London)* **429,** 47–62.
47. Reese, T. S. & Karnovsky, M. J. (1967) *J. Cell Biol.* **34,** 207–217.
48. Brightman, M. W. & Reese, T. S. (1969) *J. Cell Biol.* **40,** 648–677.
49. Crone, C. & Olesen, S. P. (1982) *Brain Res.* **241,** 49–55.
50. Butt, A. M., Jones, H. C. & Abbott, N. J. (1990) *J. Physiol. (London)* **429,** 47–62.
51. Gumbiner, B. M. (1993) *J. Cell Biol.* **123,** 1631–1633.
52. Shivers, R. R., Bowman, P. D. & Martin, K. (1985) *Tissue Cell* **17,** 417–440.
53. Wolburg, H., Neuhaus, J., Kniesel, U., Krauss, B., Schmid, E. M., Ocalan, M., Farrell, C. & Risau, W. (1994) *J. Cell Sci.* **107,** 1347–1357.
54. Tao Cheng, J. H. & Brightman, M. W. (1988) *Int. J. Dev. Neurosci.* **6,** 25–37.
55. Hirsch, M. & Noske, W. (1993) *Micron* **24,** 325–352.
56. Brightman, M. W. & Tao-Cheng, J. H. (1993) in *The Blood-Brain Barrier: Cellular and Molecular Biology*, ed. Pardridge, W. M. (Raven, New York), pp. 107–125.
57. Stoppini, L., Buchs, P. A. & Muller, D. (1993) *Neuroscience.* **57,** 985–994.
58. Clark, K. A. & Collingridge, G. L. (1995) *J. Physiol. (London)* **482,** 39–52.
59. Asztely, F. & Gustafsson, B. (1994) *Hippocampus* **4,** 148–156.
60. Collins, D. R. & Davies, S. N. (1994) *Neuropharmacology.* **33,** 1055–1063.
61. Gerfin Moser, A., Grogg, F., Rietschin, L., Thompson, S. M. & Streit, P. (1995) *Neuroscience* **67,** 849–865.
62. Sahai, S. (1990) *Eur. Arch. Psychiatry Clin. Neurosci.* **240,** 121–133.
63. Bolwig, T. G. (1988) *Acta Psychiatr. Scand. Suppl.* **345,** 15–20.
64. Cornford, E. M. & Oldendorf, W. H. (1986) *Adv. Neurol.* **44,** 787–812.
65. Deloncle, R., Guillard, O., Huguet, F. & Clanet, F. (1995) *Biol. Trace Elem. Res.* **47,** 227–233.
66. Hawkins, R. A., DeJoseph, M. R. & Hawkins, P. A. (1995) *Cell Tissue Res.* **281,** 207–214.
67. Michelson, H. B. & Wong, R. K. (1994) *J. Physiol. (London)* **477,** 35–45.
68. Medvedev, A., Mackenzie, L., Hiscock, J. J. & Willoughby, J. O. (1996) *Electroencephalogr. Clin. Neurophysiol.* **98,** 157–166.
69. de Lange, E. C., Hesselink, M. B., Danhof, M., de Boer, A. G. & Breimer, D. D. (1995) *Pharm. Res.* **12,** 129–133.
70. Westergren, I., Nystrom, B., Hamberger, A. & Johansson, B. B. (1995) *J. Neurochem.* **64,** 229–234.
71. Tossman, U. & Ungerstedt, U. (1986) *Acta Physiol. Scand.* **128,** 9–14.
72. Abercrombie, E. D. & Finlay, J. M. (1991) in *Microdialysis in the Neurosciences*, eds. Robinson T. E. & Justice, J. B., Jr. (Elsevier, Amsterdam), Vol. 7, pp. 253–274.
73. Dykstra, K. H., Hsiao, J. K., Morrison, P. F., Bungay, P. M., Mefford, I. N., Scully, M. M. & Dedrick, R. L. (1992) *J. Neurochem.* **58,** 931–940.
74. Stahle, L. (1993) *Eur. J. Drug. Metab. Pharmacokinet.* **18,** 89–96.
75. Elmquist, W. F. & Sawchuk, R. J. (1997) *Pharm. Res.* **14,** 267–288.
76. de Lange, E. C., Bouw, M. R., Mandema, J. W., Danhof, M., de Boer, A. G. & Breimer, D. D. (1995) *Br. J. Pharmacol.* **116,** 2538–2544.
77. Hammarlundudenaes, M., Paalzow, L. K. & Delange, E. C. M. (1997) *Pharm. Res.* **14,** 128–134.
78. Zhou, S. Y., Zuo, H., Stobaugh, J. F., Lunte, C. E. & Lunte, S. M. (1995) *Anal. Chem.* **67,** 594–599.